

## Effect of carbon in cobalt-silica-carbon composite catalysts for NO reduction by CO

N. Stoeva, I. Spassova\*, R. Nickolov<sup>1</sup>, G. Atanasova, M. Khristova

*Institute of General and Inorganic Chemistry, Bulgarian Academy of Sciences, 1113 Sofia, Bulgaria*

<sup>1</sup> *University of Chemical Technology and Metallurgy, 8 Kliment Ohridski Blvd., 1756 Sofia, Bulgaria*

Received: September 29, 2015; Revised December 7, 2015

Cobalt-silica-carbon composites were prepared by sol-gel method and tested as catalysts for NO reduction by CO. Active carbons of different texture parameters were used for synthesis of these composites. A cobalt-silica composite was also prepared for comparison purposes. The catalysts were characterized by low-temperature nitrogen adsorption, X-ray diffraction (XRD), and X-ray photoelectron spectroscopy (XPS) and tested in NO reduction by CO up to 300°C. Carbon-containing composites were found to exhibit a considerably higher activity in NO reduction by CO than a cobalt-silica catalyst even at low temperatures. A significant difference in transient responses between carbon-containing and carbon-free composition samples was observed revealing different rate controlling steps of the reaction. Carbon presence in cobalt-silica-carbon composites greatly influenced their microstructure including Co<sub>3</sub>O<sub>4</sub> crystalline domain size, surface area, surface composition, and oxidation state, which strongly affected catalyst performance. An increased activity could be due to cobalt sites of different oxidation state with silicon and carbon atoms in their vicinity.

**Keywords:** silica-carbon composites, sol-gel method, cobalt catalyst, NO reduction by CO.

### INTRODUCTION

NO<sub>x</sub> gases from stationary and mobile combustion sources induce a negative impact on the environment. Various methods for removing these emissions have recently been developed. Selective catalytic reduction (SCR) has been found to be an effective means for NO<sub>x</sub> removal by catalytic reduction to nitrogen in presence of reducing agents. Many active metals (Pd, Rh, Pt, Cu, Ni, Fe, Co, V, Mn, and Zn [1–4]), and catalyst preparation techniques (impregnation, sol-gel method, and coprecipitation [5–7]) have been studied. It is known that plenty of industrially applied catalysts consist of metals or metal compounds supported on a suitable support, the main role of which is to maintain the active phase in a highly divided state. However, it is proved that the role of the support is not only that of a carrier but it may contribute to the catalytic activity and can also react to some extent with other catalyst ingredients during preparation. Further, the interaction between active phase and support can affect the catalytic activity. Among many possible supports, practically only three combine an optimal chemical composition, surface area, stability, and mechanical properties, and they account for the most widely used industrial supported catalysts: alumina, silica, and carbon [8]. One of the most active catalysts for NO<sub>x</sub> elimination, that was expected to replace noble metal

catalysts, has been found to be a cobalt-based material [9–12]. In order to achieve high cobalt dispersion and reduce costs, various supports have been used, including silica, alumina, titania, and carbon. The structure of these supports and their properties, such as pore diameter, pore volume, and surface area can significantly influence cobalt dispersion and catalyst reducibility and activity/selectivity. Song and Li [13] have studied Co/SiO<sub>2</sub> catalysts with silica pore sizes of 2.4–15.8 nm and have found that larger SiO<sub>2</sub> pore sizes caused the formation of larger Co<sub>3</sub>O<sub>4</sub> crystallites, but the larger sizes also resulted in lower Co dispersion. Mesoporous silicas, MCM-41 and SBA-15, of different pore diameters [14–15] have also been selected to evaluate the effect of support porosity on cobalt dispersion. Compared with conventional metal oxide supports, active carbons (AC) display special properties, such as high purity, high mechanical strength, good electrical conductivity, and large surface area [16–19], and they are increasingly attracting considerable attention as potential supports. Fu *et al.* have found that carbon structure and cobalt dispersion determine CO conversion [20]. A high catalytic activity has been achieved by an active finely dispersed copper phase on an AC support [21]. Acidic pretreatment of the support was found to be favourable in SCR of NO<sub>x</sub> [22]. Silica is able to adsorb various gaseous and liquid compounds *via* both isolated and H-bonded surface OH groups. Wide applications of carbons are associated with surface hydrophobicity, good thermal stability, high

\* To whom all correspondence should be sent  
E-mail: ispasova@svr.igic.bas.bg

surface area, and large pore volume. It was of interest to combine a few properties of two types of material, i.e. hydrophilic silica and hydrophobic carbon, and to use the resulting material as a support for cobalt catalysts in NO reduction. A better understanding of the relationship between support features and catalytic performance of the cobalt catalyst is important for designing a better cobalt catalyst.

The objective of this study was to investigate composite catalysts based on cobalt, silica, and different ACs in the reduction of NO by CO and to find a relationship between composite porous characteristics and catalytic performance.

## EXPERIMENTAL

Sol-gel prepared cobalt-silica-carbon composites were prepared by adding  $\text{Co}(\text{NO}_3)_2$ , tetraethyl orthosilicate (TEOS), and carbon during the sol-gel process using an alkaline catalyst ( $\text{NH}_4\text{OH}$ ). TEOS,  $\text{HNO}_3$ , ethanol, and water were placed in a glass tube at room temperature and heated upon stirring to a temperature of 80–85°C under reflux conditions. The solution was kept at this temperature for 2 h. After that, the necessary amounts of metal nitrate and carbon were added into the mixture and stirred for 1 h. To obtain gel,  $\text{NH}_4\text{OH}$  was introduced to the solution. After aging for a day, the composites were dried at 120°C to obtain homogeneous solid catalysts, which were calcined at 300°C for 4 h. Inserted carbon and cobalt were 8 wt.%. Three hydrophobic active carbons (AC1, AC2, and AC3) of different texture parameters were used to prepare the catalysts, where AC1 was made of apricot shells, whereas AC2 and AC3 originated from coal and coconut shells, respectively. The samples were denoted as Co/Si-AC1, Co/Si-AC2, and Co/Si-AC3. A carbon-free catalyst, Co/Si, of the same cobalt content was prepared for comparison purposes.

Texture characteristics were determined by low-temperature (77.4 K) nitrogen adsorption on a NOVA 1200e apparatus (Quantachrome Instruments, USA). Nitrogen adsorption-desorption isotherms were analysed to evaluate specific surface areas ( $S_{\text{BET}}$ ),

based on the BET equation, and total pore volumes ( $V_t$ ), estimated in accordance with Gurvich rule. Values of micropore volume ( $V_{\text{MI}}$ ), specific surface area related to micropores ( $S_{\text{MI}}$ ), and external specific surface area ( $S_{\text{ext}}$ ) were assessed according to the V-t method [23]. Additionally, pore size distributions were calculated applying the NLDFT method using equilibrium models with cylindrical pores (for silica), a slit shape (for carbon), and slit-shaped/cylindrical pores in carbons (for silica-carbon) [24].

Powder XRD patterns were collected within the range of 10 to 80° 2 $\theta$  on a Bruker D8 Advance diffractometer with Cu  $K_\alpha$  radiation and a LynxEye detector. Average crystallite sizes were evaluated by using Scherrer equation.

XPS measurements were performed in the UHV chamber of an ESCALAB-Mk II (VG Scientific) electron spectrometer with Al  $K\alpha_{1,2}$  radiation ( $h\nu = 1486.6$  eV). The surface composition was obtained from the ratio of the corresponding intensities of C 1s, O 1s, Si 2p, Co 2p photoelectron peaks corrected by the Scofield's [25] photoionization cross-sections. The spectra were calibrated according to the Si 2p peak at 103.4 eV.

The catalytic experiments were carried out in a flow apparatus with an isothermal flow reactor in the temperature range of 20–300°C. After each catalytic measurement a temperature-programmed desorption (TPD) run at 25°C was carried out. The transient response method was used to study the interaction between gas phase and catalyst surface.

## RESULTS AND DISCUSSION

Table 1 presents adsorption properties of initial carbon materials and prepared composites.

Texture parameters of the initial ACs as specific surface area, pore volume, and micro-meso porosity are quite different. The resulting composites have specific surface areas more close to the cobalt-silica composite than to AC ingredients. However, addition of carbon led to increased  $S_{\text{BET}}$  and decreased  $V_t$  compared to the pure cobalt-silica. Carbon microporosity reflected strongly micropore availability of

**Table 1.** Texture parameters of active carbons, cobalt-silica, and cobalt-silica-carbon composites

Sample	$S_{\text{BET}}$ $\text{m}^2\text{g}^{-1}$	$S_{\text{ext}}$ $\text{m}^2\text{g}^{-1}$	$V_t$ $\text{cm}^3\text{g}^{-1}$	$V_{\text{mi}}$ $\text{cm}^3\text{g}^{-1}$	$V_{\text{mes}}$ $\text{cm}^3\text{g}^{-1}$	$V_{\text{mi}}/V_{\text{mes}}$	$D_{\text{av}}$ nm
AC1	700	158	0.38	0.22	0.16	1.38	2.2
AC2	804	183	0.50	0.25	0.25	1.00	2.5
AC3	1108	232	0.55	0.38	0.17	2.24	1.9
Co/Si-AC1	553	222	0.34	0.14	0.20	0.70	2.5
Co/Si-AC2	579	418	0.39	0.07	0.32	0.22	2.7
Co/Si-AC3	565	199	0.30	0.16	0.14	1.14	2.1
Co/Si	533	349	0.30	0.08	0.22	0.35	2.4

the composites. For the Co/Si-AC2 composite, the main part of the pore volume belonged to the mesoporous space with a minor contribution of micropores. Additionally, this sample had the highest specific surface area and pore volume.

Figure 1 displays adsorption-desorption isotherms (a) and pore size distribution (PSD) curves (b) of the composites (shifted). One can see differences in porous texture.

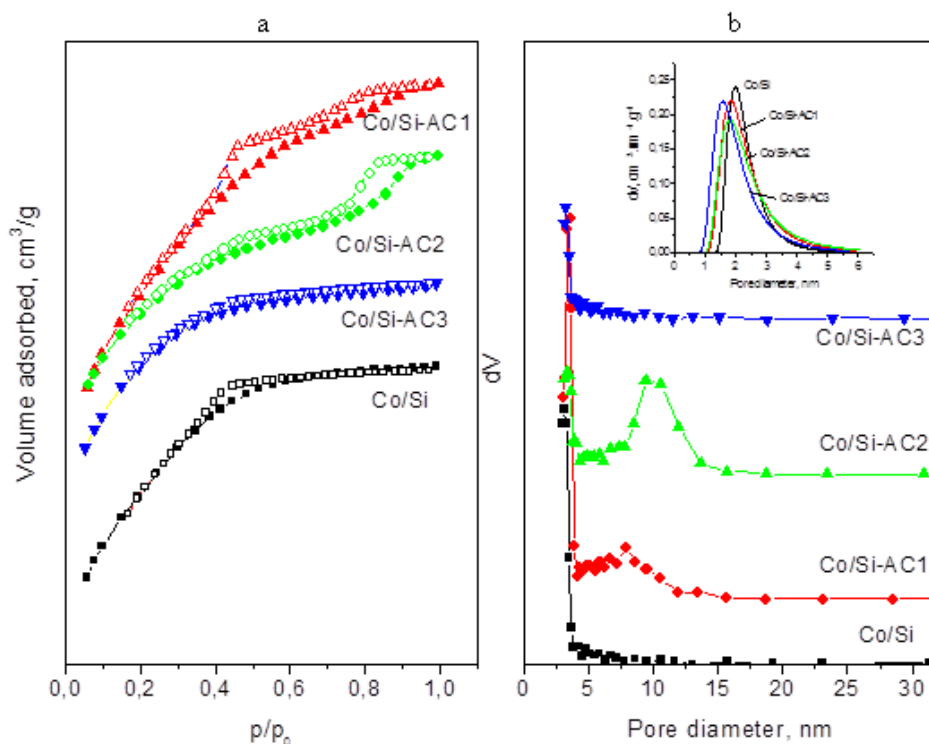
The adsorption-desorption isotherms are of the I/IV type according to IUPAC classification. They reveal influence of texture parameters of the ACs modifiers on the sol-gel process in presence of cobalt. The role of the cobalt salt in the process is most clearly evident with the Co/Si sample, which is a fine mesopore material, so Co is related primarily to reducing mesopore size (Fig. 1b), as also reported in Ref. [26]. AC3 is a micro-mesoporous material having the highest specific surface and external area whereas Co/Si-AC3 was a composite of the most developed microporosity due to AC3 contribution. The slope in the isotherm is a result of adsorption along with capillary condensation on the external surface. The hysteresis loops observed with Co/Si-AC2 and Co/Si-AC1 indicate at least a bidisperse mesoporous texture due to conflicting contribution of the two modifiers: cobalt and active carbon. One could suggest that if cobalt contributed to a fine pore formation, AC might have led to larger pores including formation of globules on the external

surface. As used ACs could sorb cobalt ions, they counteracted the effect of Co and caused the occurrence of areas of different thickness.

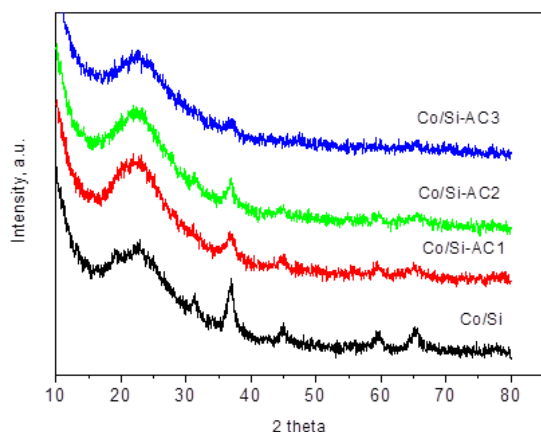
XRD data are shown in figure 2. The diffraction pattern at around  $22.5^\circ$  with a broad peak could be attributed to amorphous silica with a contribution of broad diffraction features due to a turbostratic structure of disordered carbon (expected at  $26.5^\circ$ ).

A Co/Si sample (PDF 71-4921) with crystallite sizes of  $\sim 10$  nm demonstrates well-defined reflections, which are typical of  $\text{Co}_3\text{O}_4$ :  $2\theta$   $19.1^\circ$ ,  $31.45^\circ$ ,  $37.06^\circ$ ,  $45.07^\circ$ ,  $59.71^\circ$ ,  $65.64^\circ$ . No shift of diffraction peaks was observed with respect to a conventional  $\text{Co}_3\text{O}_4$  spinel indicating that no Si-containing solid solution has been formed. At the same time, small reflections, typical of  $\text{Co}_3\text{O}_4$ , were registered for the AC-containing samples, probably due to higher Co dispersion (Fig. 2) and smaller particle sizes. The average diameter of the crystallites in these cases, based on calculations by Scherrer equation, was about 6–7 nm, thus indicating higher dispersion of the cobalt particles in the carbon-containing composites.

XPS measurements were carried out to investigate the presence, content, and chemical state of silicon, carbon, cobalt, and oxygen in the samples. Surface compositions derived from respective peak areas are given in Table 2. XPS spectra of Si 2p and O 1s (not presented) indicate that these elements are mainly in the  $\text{SiO}_2$  oxide form.



**Fig. 1.** Adsorption-desorption isotherms (a) and pore size distribution (b) of synthesized composites.



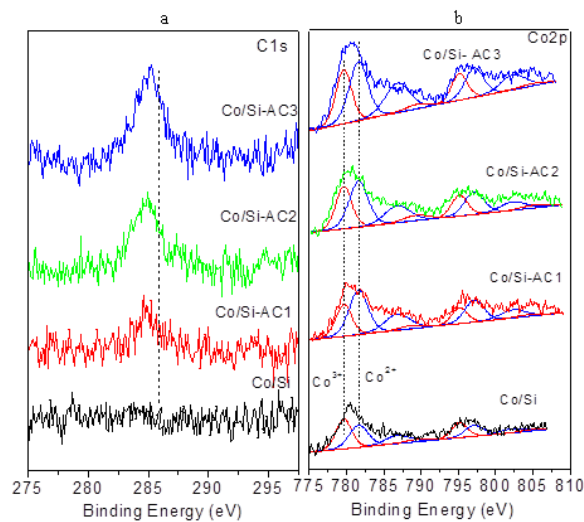
**Fig. 2.** XRD patterns of cobalt-silica-carbon and cobalt-silica composites.

Figure 3 discloses XPS spectra of C 1s (a) and Co 2p (b) of the investigated catalysts. For the cobalt-silica-carbon composites, one peak at 284.8 eV was registered in the C 1s spectra. Binding energies (BEs) of about 284.8–285.2 eV could be attributed to overlapping peaks of  $sp^2$ - and  $sp^3$ -hybridized as well as adventitious carbon phases [27]. Evaluation of Co 2p narrow scans allows assigning cobalt oxidation state.  $Co^{2+}$  and  $Co^{3+}$  ions could be distinguished by the binding energies and intensities of shakeup peaks. Whereas  $Co^{3+}$  ions show only very weak shakeup peaks with a main signal at  $\sim 791$  eV,  $Co^{2+}$  has pronounced shakeup peaks at about 785 and 801 eV [28]. The binding energies of the Co  $2p_{3/2}$  and Co  $2p_{1/2}$  peaks are at 780.4 and 795.9 eV, respectively, with splitting energies at 15.5 eV indicating that  $Co_3O_4$  has been mainly in the form of a spinel phase [29, 30]. The Co 2p spectra were further deconvoluted into  $Co^{2+}$  and  $Co^{3+}$ , respectively. Co 2p peaks at  $\sim 779.6$ , 789.3, 795.1, and 804.8 eV are characteristic of  $Co^{3+}$ , while the peaks at 781.6, 786.8, 797.1, and 802.3 eV correspond to  $Co^{2+}$ .

Shakeup satellites at about 787.1 eV, the latter being an intermediate value compared with that for CoO (785 eV) and  $Co_3O_4$  (789 eV) [28], indicate a higher presence of  $Co^{2+}$  species on the surface compared to stoichiometric  $Co_3O_4$  (Fig. 3 and Table 2). Such a surface enrichment in  $Co^{2+}$  has been registered for cobalt-silica catalysts [31]. However, the AC containing composites have more  $Co^{2+}$  species evidencing a reductive role of the carbon along with supporting higher dispersion of the cobalt particles (Fig. 3 and Table 2).

XPS studies indicate that cobalt ion distribution over the surface and into the bulk is dependent on carbon ingredient type used and micro-mesoporous space formed. Cobalt particles penetrate into the bulk if the mesopore volume is higher (Co/Si-AC2)

and stay on the surface if the micropore space is significant (Co/Si-AC1 and Co/Si-AC3). The highest cobalt-rich surface was that of Co/Si which is logical bearing in mind its fine porous structure hindering cobalt penetration. Hence, carbon presence has influence on cobalt distribution between surface and the bulk. These results confirm data on adsorption measurements. Quantitative XPS results showed that the molar Si/Co ratio at the surface was much higher than that of the bulk. The same tendency was observed for carbon confirming that most of the silica was on the surface of the catalysts.



**Fig. 3.** XPS spectra of C 1s (a) and Co 2p (b) of cobalt-silica-carbon and cobalt-silica composites.

**Table 2.** Surface compositions derived from XPS

Sample	C, at. %	O, at. %	Si, at. %	Co, at. %	$Co^{3+}/Co^{2+}$
Co/Si-AC1	3.5	60.2	35.7	0.6	0.61
Co/Si-AC2	4.1	59.3	35.7	0.9	0.48
Co/Si-AC3	2.4	62.4	34.2	1.0	0.55
Co/Si	–	63.7	34.8	1.5	0.89

Figure 4 illustrates a temperature dependence of NO conversion degree and the respective TPD profiles. The investigation showed that the reduction of NO by CO proceeded to nitrogen, i.e. no  $N_2O$  was registered in the whole temperature interval. The cobalt-silica catalyst was slightly active whereas carbon addition led to a significant increase in catalytic activity: all cobalt-silica-carbon catalysts manifested a high activity by CO toward NO even at  $100^\circ C$ . Co/Si-AC2 demonstrated a 70% conversion of NO to nitrogen at  $200^\circ C$  and almost 100% activity at  $300^\circ C$ . TPD spectra of NO indicated no desorption from Co/Si. The carbon-containing samples desorbed NO in the temperature range of  $100$ – $250^\circ C$ . It is evident that they desorbed different amounts of NO. One broad NO desorption peak for

Co/Si-AC1 and Co/Si-AC2 is available in the upper interval considering a variety of NO adsorbed species, while for Co/Si-AC3 two distinct desorption peaks are observed. The amount of desorbed NO from Co/Si-AC1 and Co/Si-AC2 was more than that with Co/Si-AC3, which coincides with the order of activity of the investigated samples. The role of composite texture was decisive. It can be seen in figure 1b and table 1 that enhanced  $V_{mes}$  enables better mass transfer of reagents and products.

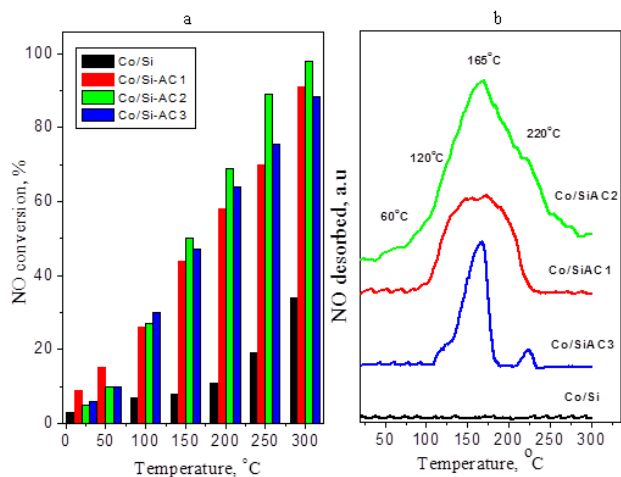


Fig. 4. Temperature dependence of NO conversion degree (a) and TPD spectra of NO (b).

Figure 5 displays response curves of the NO and CO reagents and  $N_2$  and  $CO_2$  products at a temperature of 50, 100, 200, and 300°C. Differences in the curves reveal different rate-controlling steps of the reaction over the catalysts and a change in the rate-controlling step is associated with a change of reaction mechanism. A significant difference in the response curves was observed for samples with and without AC in the composition. The response curves for NO and CO at 50°C on Co/SiAC1 and Co/SiAC2 are of an overshoot type, while responses of Co/Si and Co/SiAC3 are of a momentous and monotonically growing type. The overshoot response indicates that the rate-limiting step is concurrent adsorption of the reagent or regeneration of the active centres. With the less active cobalt-silica-carbon catalyst, an overshoot response appeared only at 200°C. The momentous response shows that the rate-limiting step is associated with surface reaction or adsorption of the reagents. The monotonically growing type response reveals that a combination between surface reaction and product slow desorption is the rate-limiting step. NO and CO desorption curves of Co/SiAC3 at temperatures up to 200°C at stop-stages show that the rate-limiting step is related to adsorption of the reagents and their slow desorption. The results of transient responses support the TPD studies presented above.

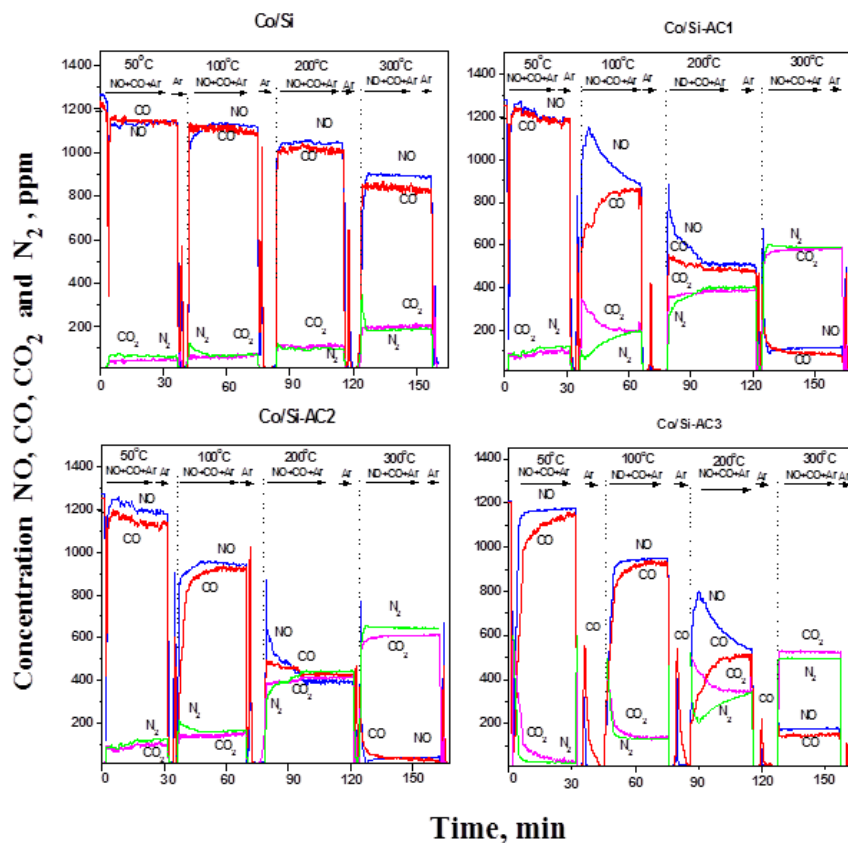


Fig. 5. Transient response curves of NO, CO, CO<sub>2</sub>, and N<sub>2</sub>.

Carbon presence in the support strongly affects the formation of a cobalt-containing active phase. AC contributes to the formation of partially reduced highly dispersed surface cobalt species which manifest a high catalytic activity and selectivity for NO reduction by CO. A relatively low catalytic activity observed for Co/Si can be related probably to a strong interaction between partially reduced  $\text{Co}^{2+}$  species under the reaction medium and the silica support and is dependent on crystallite size. The nature of carbon affects composite texture, micro- and mesopores, and pore volume. Generally,  $\text{Co}^{3+}$  on the catalyst surface is thought to provide the active sites for NO reduction while  $\text{Co}^{2+}$  is considered inactive and the possible reaction pathway on  $\text{Co}_3\text{O}_4$  follows a redox type reaction mechanism. However, with the nanocomposites the surface is rich in silica and  $\text{Co}^{2+}$  species compared with normal  $\text{Co}_3\text{O}_4$ , which may suggest that  $\text{Co}^{3+}$  is not the only active species for NO reduction. Zhang *et al.* reported a high activity and selectivity of  $\text{Co}_3\text{O}_4$  for NO reduction by CO on a preferentially exposed surface restructured into nonstoichiometric  $\text{CoO}_{1-x}$  nanorods [32]. The same was observed for NO reduction by  $\text{C}_2\text{H}_4$  [33], CO oxidation [34], and  $\text{N}_2\text{O}$  decomposition [35].

#### CONCLUSION

Cobalt-silica-carbon composites exhibit a considerably higher activity in NO reduction by CO than cobalt-silica catalyst even at low temperatures. The presence of carbon greatly influences the microstructure (including crystalline size of  $\text{Co}_3\text{O}_4$ , surface area, surface composition, and oxidation state) of the cobalt-silica-carbon composites, which may strongly affect catalyst performance. An increased activity could be due to cobalt sites of different oxidation state with Si and C atoms in their vicinity.

*Acknowledgements: This work was financially supported by the European Social Fund through Grant BG051PO001-3.3.06-0050 and by the Bulgarian Science Fund (Grant E02/2- 2014).*

#### REFERENCES

- G. M. Tonetto, M. L. Ferreira, D. E. Damiani, *J. Mol. Catal. A-Chem.*, **193**, 121 (2003).
- P. S. Dimick, J. L. Kross, E. G. Roberts, R. G. Herman, H. G. Stenger, C. E. Lyman, *Appl. Catal. B-Environ.*, **89**, 1 (2009).
- H. H. Tseng, H. Y. Lin, Y. F. Kuo, Y. T. Su, *Chem. Eng. J.*, **160**, 13 (2010).
- J. Zhu, F. Gao, L. Dong, W. Yu, L. Qi, Z. Wang, L. Dong, Y. Chen, *Appl. Catal. B-Environ.*, **95**, 144 (2010).
- C. Y. Lu, M. C. Wei, S. H. Chang, M. Y. Wey, *Appl. Catal. A-Gen.*, **354**, 57 (2009).
- X. Gao, Y. Jiang, Y. Zhong, Z. Luo, K. Cen, *J. Hazard. Mater.*, **174**, 734 (2010).
- F. Zhang, S. Zhang, N. Guan, E. Schreier, M. Richter, R. Eckelt, R. Fricke, *Appl. Catal. B-Environ.*, **73**, 209 (2007).
- F. Rodriguez-Reinoso, *Carbon*, **36** (3), 159 (1998).
- B. Meng, Z. Zhao, X. Wang, J. Liang, J. Qiu, *Appl. Catal. B-Environ.*, **129**, 491 (2013).
- X. Chen, J. Zhang, Y. Huang, Z. Tong, M. Huang, *J. Environ. Sci.*, **21**, 1296 (2009).
- A. E. Palomares, A. Uzcátegui, A. Corma, *Catal. Today*, **137** (2–4), 261 (2008).
- F. Lónyi, J. Valyon, L. Gutierrez, M. A. Ulla, E. A. Lombardo, *Appl. Catal. B-Environ.*, **73** (1–2), 1 (2007).
- D. Song, J. Li, *J. Mol. Catal. A-Chem.*, **247**, 206 (2006).
- A. Y. Khodakov, A. Griboval-Constant, R. Bechara, F. Villain, *J. Phys. Chem. B*, **105**, 9805 (2001).
- H. F. Xiong, Y. H. Zhang, K. Y. Liew, J. L. Li, *J. Mol. Catal. A-Chem.*, **295**, 68 (2008).
- R. Q. Long, R. T. Yang, *Ind. Eng. Chem. Res.*, **40**, 4288 (2001).
- M. Hussain, J. S. Yun, S. K. Ihm, N. Russo, F. Geobaldo, *Ind. Eng. Chem. Res.*, **50**, 2530 (2011).
- Y. H. Hu, E. Ruckenstein, *Ind. Eng. Chem. Res.*, **43**, 708 (2004).
- C. H. See, A. T. Harris, *Ind. Eng. Chem. Res.*, **46**, 997 (2007).
- T. Fu, J. Lv, Z. Li, *Ind. Eng. Chem. Res.*, **53**, 1342 (2014).
- C. Y. Lu, M. Y. Wey, Y. H. Fu, *Appl. Catal. A-Gen.*, **344**, 36 (2008).
- K.-H. Chuang, C.-Y. Lu, M.-Y. Wey, Y.-N. Huang, *Appl. Catal. A-Gen.*, **397**, 234 (2011).
- B. C. Lippens, J. H. de Boer, *J. Catal.*, **4**, 319 (1965).
- A. V. Neimark, P. I. Ravikovitch, *Micropor. Mesopor. Mater.*, **44/45**, 697 (2001).
- J. Scofield, *J. Electron. Spectrosc. Relat. Phenom.*, **8**, 129 (1976).
- G. A. Santos, C. M. B. Santos, S. W. da Silva, E. A. Urquieta-González, P. P. Confessori Sartoratto, *Colloids Surf. A-Physicochem. Eng. Aspects*, **395**, 217 (2012).
- M. V. Sopinsky, V. S. Khomchenko, V. V. Strelchuk, A. S. Nikolenko, G. P. Olchovyk, V. V. Vishnyak, V. V. Stonis, *Nanoscale Res. Lett.*, **9**, 182 (2014).
- A. D. Pandey, C. Jia, W. Schmidt, M. Leoni, M. Schwickardi, F. Schüth, C. Weidenthaler, *J. Phys. Chem. C*, **116**, 19405 (2012).
- S. W. Ho, M. Houalla, D. M. Hercules, *J. Phys. Chem.*, **94**, 6396 (1990).
- H. A. E. Hagelin-Weaver, G. B. Hoflund, D. M. Minahan, G. N. Salaita, *Appl. Surf. Sci.*, **235**, 420 (2004).
- C.-J. Jia, M. Schwickardi, C. Weidenthaler, W. Schmidt, S. Korhonen, B. M. Weckhuysen, F. Schüth, *J. Am. Chem. Soc.*, **133**, 11279 (2011).
- S. Zhang, J. Shan, Y. Zhu, L. Nguyen, W. Huang, H. Yoshida, S. Takeda, F. Tao, *Nano Lett.*, **13**, 3310 (2013).

33. X. Chen, A. Zhu, C. Shi, *Catal. Lett.*, **133**, 134 (2009).  
34. J. Li, G. Lu, G. Wu, D. Mao, Y. Guo, Y. Wang, Y. Guo, *RSC Adv.*, **3**, 12409 (2013).  
35. L. Xue, C. Zhang, H. He, Y. Teraoka, *Appl. Catal. B- Environ.*, **75**, 167 (2007).

## ВЛИЯНИЕ НА ВЪГЛЕРОДА В КОБАЛТ-СИЛИКАТНО-ВЪГЛЕРОДНИ КОМПОЗИТНИ КАТАЛИЗАТОРИ ЗА РЕДУКЦИЯ НА NO С CO

Н. Стоева, Ив. Спасова\*, Р. Николов<sup>1</sup>, Г. Атанасова, М. Христова

*Институт по обща и неорганична химия, Българска академия на науките, 1113 София, България*

<sup>1</sup> *Химико-технологичен и металургичен университет, Бул. „Климент Охридски“ 8, 1756 София, България*

Постъпила на 29 септември 2015 г.; Преработена на 7 декември 2015 г.

(Резюме)

Кобалт-силикатно-въглеродни композити са получени по зол-гел метод и са тествани като катализатори за редукция на азотен оксид с въглероден оксид. Активни въглени с различни текстурни параметри са използвани за синтез на композитите. За сравнение е получен кобалт-силикатен композит. Катализаторите са охарактеризирани посредством нискотемпературна адсорбция на азот, рентгенова дифракция (XRD), рентгенова фотоелектронна спектроскопия (XPS) и тествани за редукция на NO с CO при температури до 300°C. Намерено е, че въглерод-съдържащите композити показват значително по-добра активност от кобалт-силициево оксиден катализатор при редукция на NO с CO дори при ниски температури. Наблюдава се значителна разлика във вида на кривите на отклик на образците с и без въглерод, разкриваща различни определящи скоростта етапи при тях. Наличието на въглерод влияе значително на микроструктурата (включително размер на Co<sub>3</sub>O<sub>4</sub> кристали, специфична повърхност, повърхностен състав и окислително състояние) на кобалт-силикатно-въглеродните композити, което се отразява върху каталитичната им активност. Повишената активност вероятно се дължи на кобалтови йони в различни окислителни състояния в близост до силициеви и въглеродни атоми.